TELKOMNIKA, Vol.13, No.2, June 2015, pp. 670 ~ 677
ISSN: 1693-6930, accredited A by DIKTI, Decree No: 58/DIKTI/Kep/2013
DOI: 10.12928/TELKOMNIKA.v13i2.999

Water Model Study on Removing Inclusion from Molten Steel by Bubble Attachment in RH Degasser

Chunjie Yang*, Fuping Tang, Minggang Shen
University of Science and Technology Liaoning,
Anshan City 114053, Liaoning, China
*Corresponding author, e-mail: chunjieyang_tel@163.com

Abstract

In this paper, a water model is established, at geometric similarity ratio of 1:4, to simulate a real 180-t RH vacuum refining device. Removing inclusion from molten steel by bubble attachment in RH degasser is analyzed using the water model. The effects of variables such as bubble size, treatment time, life-gas flow rate, amount and time of NaHCO3 addition are investigated by using high speed video and image-process software.

***Keywords**: Bubble Attachment, Inclusion, Water Model, RH Degasser*

1. Introduction

Technologies for clean steelmaking are being continuously developed to meet the ever increasing demands on material properties [1]. The composition, quantity and size distribution of non-metallic inclusions are all important in influencing the physical properties of steel. Inclusions in steel greatly affect its physical and chemical properties, such as fatigue life, machinability and corrosion resistance [2]. The big size (diameter more than 50μm) inclusions are removed primarily by Stokes floating. However, inclusions less than 50 μm in diameter cannot rise rapidly and they tend to remain in the steel [3]-[5]. Oxide inclusions are lighter than molten steel and can float up to the slag surface, stick to the wall, or stick to bubbles and be transported to the surface [6]. Some solid inclusions, such as alumina and silica, are not wetted by the liquid steel and therefore can be removed by attachment to gas bubbles [7].

In order to satisfy the requirements for the degree of cleanliness in steel, controlling the amount, size distribution and shape of inclusions is of great important in the steelmaking process. The formation, modification and removal of these inclusions in liquid steel is controlled by the various processing units [8]. As one of the important refining equipments between steelmaking and continuous casting, RH vacuum refining plays an important role in removing the inclusions in the molten steel. RH refining process, to a significant degree, has become a main refining operation for removing inclusions from liquid steel in order to minimize the inclusions that could potentially form defects in the finished product or adversely affect the product properties [1],[9].

During steel secondary refining, aided by surface tension forces from non wetting contact, most solid inclusions tend to collect on surfaces such as bubbles [10]-[11].Therefore, special methods have been developed to remove non-metallic inclusions from molten steel [12]-[13]. Miki and Thomas developed a mathematical model to predict the removal of alumina inclusions from molten steel in a continuous casting tundish. Although several papers have been written on inclusion removal by gas bubbles flotation in water modeling [14]-[17].

However, there are few papers systematically studying the fundamentals of inclusion removal by bubble attachment in liquid steel in RH vacuum degasser and the effects of bubble size, treatment time, life-gas flow rate etc.

This paper presents fundamental models to quantify the removal of inclusions by bubbles in molten steel. A water model is used to study the influencing the removal of fine inclusions(<50 μm diameter) in a 180-t RH vacuum refiner.

Received November 14, 2014; Revised February 25, 2015 Accepted March 12, 2015

2. Experimental Principle and Method

To make the prototype and the model identical in both geometry and dynamics, a water model of a 180-t RH vacuum degasser was established with a geometric similarity ratio of 1:4. Table 1 shows the operational and geometrical parameters of the prototype and the physical model.

Table 1. Main parameters of the prototype and the physical model (in mm)

Equipment	Dimensions	Prototype	Model
Ladle	Height	4428	1107
	Lower internal diameter	3244	811
	Lower internal diameter	2656	664
	Liquid level	4000	1000
Vacuum vassel	Internal diameter	1960	490
	Height	3852	963
Snorkel	Length	1660	415
	Internal diameter	560	140

A diagram of the experimental apparatus is shown in Figure 1. Liquid steel was simulated by 400L of acidified water, and fine inclusions by 20g of high-density polypropylene beads (40~50 μm diameter or so), and compressed air was used as the lift gas. The inclusions are put into 500ml water in a beaker and stirred using an ultrasonic stirrer to make sure the inclusions were fully wetted. The water with inclusions is then transferred into the experimental vessel.

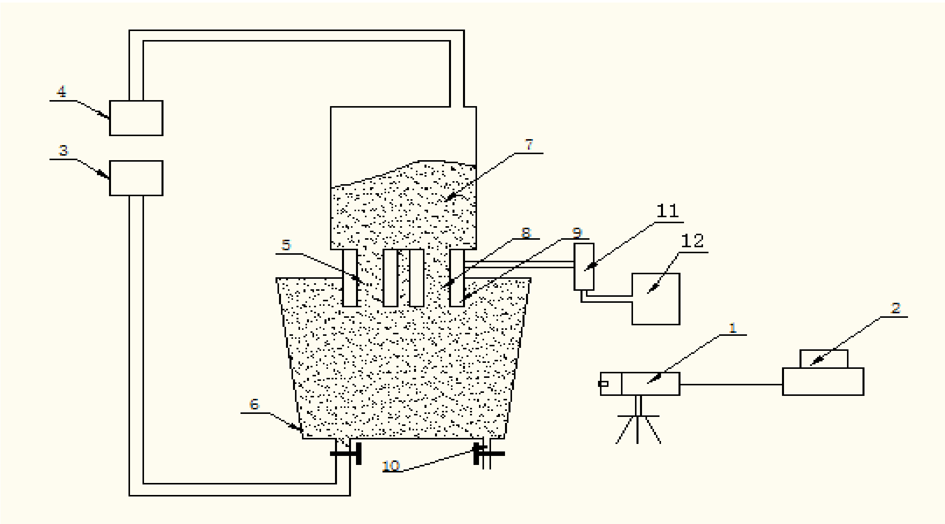

Figure 1. Schematic drawing of the experimental apparatus

1—high speed video; 2—computer; 3—water tank; 4—vacuum pump; 5—downleg snorkel; 6—ladle; 7—vacuum chamber; 8—upleg--snorkel; 9—distribution chamber for lift-gas ;10—valve; 11—velocity-meter; 12—air cylinder

The size (μm) distribution curve of inclusion are shown in Figure 2.

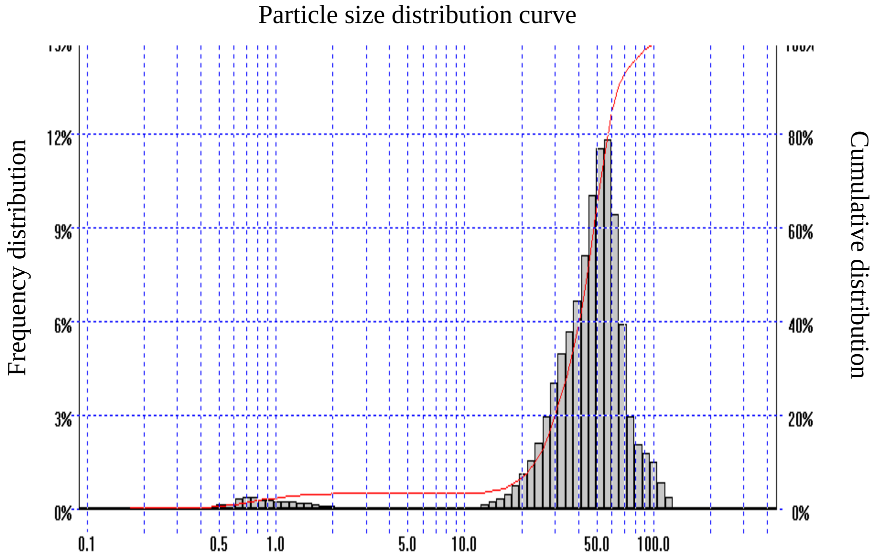

Figure 2. inclusion's particle size distribution curve

Sahai and Emi[18] give the following relationship:

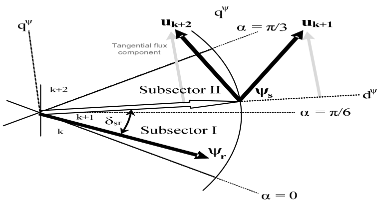

(1)

Where R —is the radius, λ —is the geometric similarity ratio, ρ —is the density, and the subscripts inc, m, p, st and w indicate values for inclusions, model, prototype, liquid steel and NaCl solution, respectively.

The relevant parameters of the media (namely, the densities ρ of the liquid and the inclusions) for the model and prototype are shown in Table 2.

Table 2. Relevant parameters of the media for the model and prototype

Density	Prototype	Model
ρ_{liquid}/kg m^{-3}	7.0×10^{3} (steel)	1.06×10^{3}
ρ_{inc}/ kg m^{-3}	3.9×10^{3} (Al_2O_3) or or 2.7×10^{3} (SiO_2)	0.91×10^{3}(polypropylene)

The contact angle of the inclusions with water is 118°, The morphology of the inclusions in the water model are shown in Figure 3.

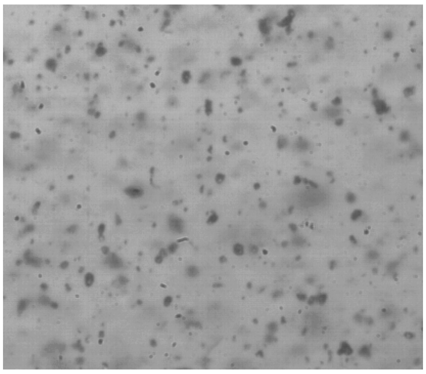

Figure 3. Morphology of the polypropylene beads in the water model

Substitution of λ =0.25 and the parameters from Table 2 into equation (1) gives the relationships between the diameters D of the inclusions in the model and in the prototype. For Al_2O_3 inclusions.

$$\frac{Rinc,m}{Rinc,p}=\frac{Dinc,m}{Dinc,p}=1.2509 \quad (1)$$

and so

$$Dinc,p=\frac{Dinc,m}{1.2509} \quad (2)$$

For SiO_2 inclusions,

$$\frac{Rinc,m}{Rinc,p}=\frac{Dinc,m}{Dinc,p}=1.4733 \quad (3)$$

and so

$$Dinc,p=\frac{Dinc,m}{1.4733} \quad (4)$$

Therefore, according to equations (2) and (4), polypropylene beads of diameter 40 μm can be used to simulate 31.98 μm diameter Al_2O_3 inclusions or 27.15 μm diameter SiO_2 inclusions.

The inclusion removal rate after the first *j* time intervals is calculated from the formula

$$\eta_j=\frac{\sum_{i=1}^{j} m_{ti}}{m_0} \quad (5)$$

Where m_{ti} is the removal amount of inclusion in the *i*th time interval, and m_0 is the total amount of inclusions.

Acidified $NaHCO_3$ was used to produce fine bubbles of CO_2 according to the reaction

$$NaHCO_3 + H^+ \rightarrow Na^+ + H_2O + CO_2\uparrow \quad (6)$$

Bubble shape changes with size. The aspect ratio of the bubble e varies according to the following empirical relationship [19]:

$$e = 1 + 0.163Eo^{0.757} \tag{7}$$

where Eo is the Eötvös number, which represents the ratio between the buoyancy and surface tension forces. Bubbles small than 3 mm are spherical, bubbles 3 to 10 mm are spheroidal, and bubbles larger than 10 mm are spherical-cap shaped[20-22]. Almost all of bubbles produced by adding $NaHCO_3$ to acidified water are spherical due to their size of 0.5~1.5mm. The morphology of bubble in the water model was shown in Figure 4.

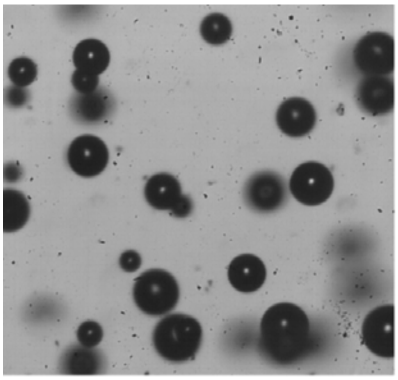

Figure.4. Morphology of bubble in the water model

The influence on the inclusion removal rate of treatment time, flow rate and method of addition of lift-gas, and amount and time of $NaHCO_3$ addition were examined.

3. Results and discussion

3.1. Process of Inclusions Adhered to Bubble

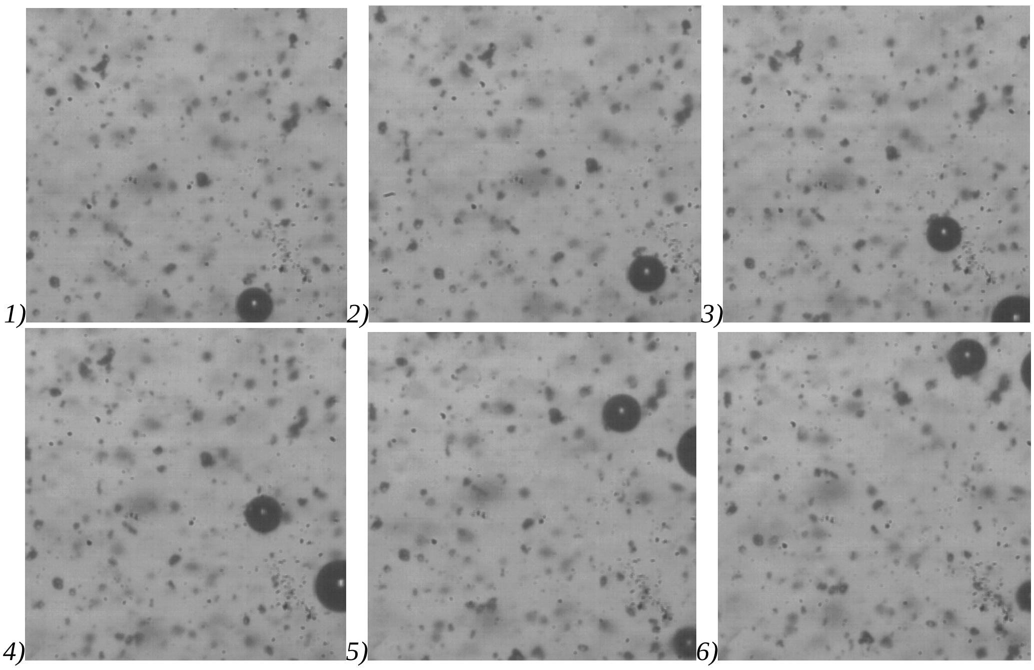

Figure 5. The process of inclusions adhered to bubble

The process of inclusions adhered to bubble is showed in Figure 5. The attachment process can be decomposed into 5 sub-processes which the particle approaches and collides the gas bubble, the thin film of liquid between the particle and the bubble is formed, the new interface of gas-solid appears after the thin film decreases to less than a critical thickness and ruptures, the inclusion slips to the bottom on the bubble surface, and the inclusion follows the bubble in dynamic and stable state to floating up finally.

Finer bubbles provide a larger gas/liquid interfacial area and higher attachment probability of inclusions to bubbles [23]. Inclusions tend to pass the midpoint of the bubble and first touch the bubble surface toward the bottom side. If the normal distance from the inclusion center to the surface of the bubble quickly becomes less than the inclusion radius then collision attachment takes place [24].

It can be concluded that the smaller bubbles have a greater rate of inclusions removal. This conclusion is in agreement with Zhang's fundamental analysis [23]-[26]. The average equivalent size of bubbles is estimated to be 0.5~1.5mm in diameter in the mold investigated in this work.

3.2. Effect of treatment time on inclusion removal rate

The relationship between inclusion removal rate and treatment time is show in Figure 6. The inclusion removal rate increased gradually with increasing treatment time, and most inclusions were removed between 0 and 15 min.

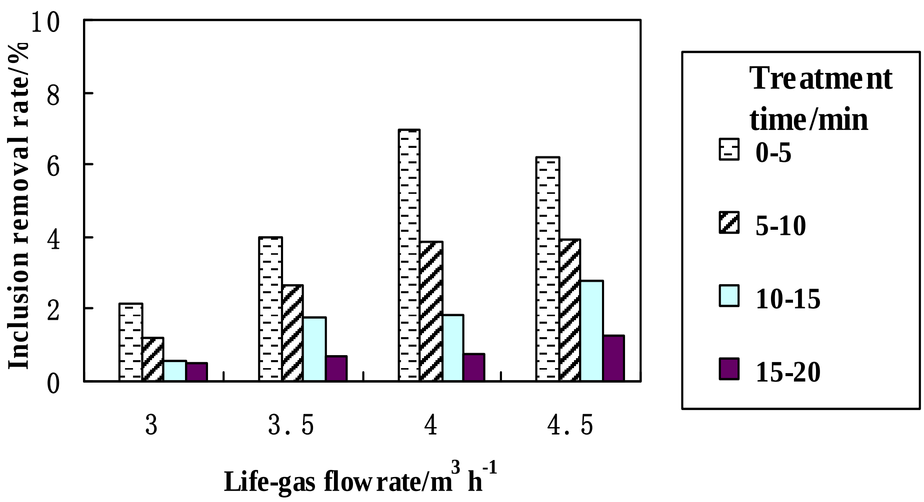

Figure 6 . Relationship between inclusion removal rate and treatment time

3.3. Effect of lift-gas flow rate on inclusion removal rate

As can be seen from Figure 7, for a treatment time of 20 min, the inclusion removal rate increased rapidly as the lift-gas flow rate was raised from 3.0 m^3 h^{-1} to 5.0 m^3 h^{-1} , after which it tended to stabilize.

With increasing lift-gas flow rate, the circulation rate initially increases, and consequently so does, the inclusion removal rate. However, if the lift-gas flow rate becomes too large, the flow pattern of the liquid steel is altered. Over-rapid flow of liquid steel inhibits the floation and removal of inclusions. There is therefore an optimum value of the life-gas flow rate: in this experiment, the inclusion removal rate was greatest when the lift-gas flow rate was about 4.5 m^3 h^{-1}.

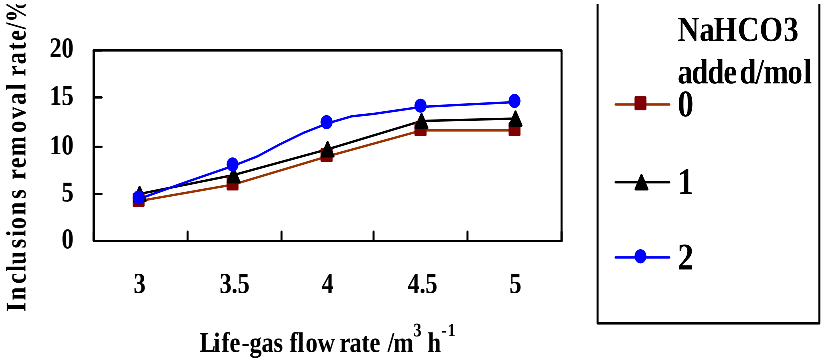

Figure. 7 . Relationship between inclusion removal rate and lift-gas flow rate

3.4. Effect of amount and time of $NaHCO_3$ addition on inclusion removal rate

Figure 8 shows the relationship between inclusion removal rate and the amount and time of $NaHCO_3$ addition for a treatment time of 20 min and the optimum value of the lift-gas flow rate 4.5 m^3 h^{-1}. It can be seen that the inclusion removal rate increased gradually with the addition of greater amounts of $NaHCO_3$, although, under conditions of industrial production, to avoid the introduction of excessive amounts of impurities, various factors need to be considered. The effect is was greatest when the $NaHCO_3$ was at the beginning.

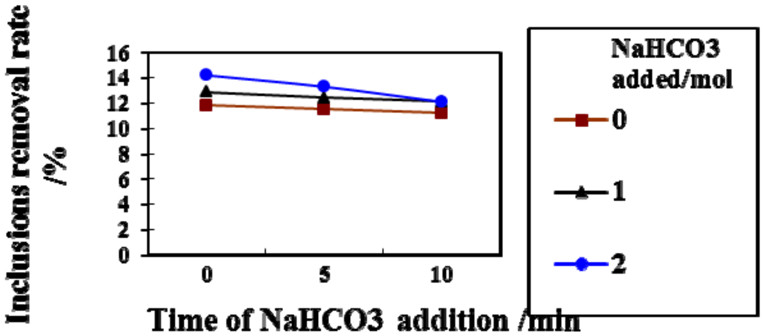

Figure.8. Relationship between inclusion removal rate and amount and time of $NaHCO_3$ addition

4. Conclusions

The influences of treatment time, lift-gas flow rate and amount and time of $NaHCO_3$ addition on the inclusion removal rate have been investigated using a water model of 1:4 linear scale for a 180-t RH-TB degasser. The following conclusions can be drawn from the results:

1. The inclusion removal rate increases gradually with increasing treatment time, with most inclusions being removed between 5 and 18 min. In this water model experiment, the treatment time was chosen as 20 min to obtain the best effect.
2. The inclusion removal rate increases with increasing lift-gas flow rate until an optimum value is reached, which in this experiment was 4.5 m^3 h^{-1}.
3. The inclusion removal rate increases gradually with the addition of $NaHCO_3$, and the effect is greatest when all of the $NaHCO_3$ is added at the beginning.
4. The smaller bubbles have a greater rate of inclusions removal. The average equivalent size of bubbles is estimated to be 0.5~1.5mm in diameter in the mold investigated in this work.

References

[1] P Kaushik, M Lowry, H Yin, H Pielet. Inclusion Characterisation for Clean Steelmaking and Quality Control. *Ironmaking and Steelmaking.* 2012; 39: 284-300.
[2] J Cheng, R Eriksson, P Jonsson. Determination of macroinclusions during clean steel production. *Ironmaking Steelmaking.* 2003; 30: 66–72.
[3] R Dekkers. Non-metallic inclusions in Liquid Steel. *PhD thesis.* Katholieke Universiteit Leuven. 2002. available at http://members.home.nl/rob.dekkers/pdf-files/contents.pdf
[4] AW Cramb. *Inclusion formation and removal.* August 1998. Available at http://neon.mems.cmu.edu/afs/afs2/form.html.
[5] LF Zhang, BG Thomas. Proc. 7th European Electric Steelmaking Conf., Venice, Italy. May. 2002: 277–286.
[6] M Söder. Growth and removal of inclusions during ladle stirring. *Licentiate Thesis.* Royal Institute of Technology, Stockholm, Sweden. 2000.
[7] F Tang, Z Li, X Wang, B Chen, P Fei. Cleaning IF molten steel with dispersed in-situ heterophases induced by the composite sphere explosive reaction in RH ladles. *Int. J. Miner. Metall. Mater*. 2011; 18: 144–149.
[8] CJ Treadgold. Behaviour of Inclusion in RH Vacuum degasser. *Ironmaking and Steelmaking*. 2003; 30: 120-124.
[9] JH Wei, HT Hu. Mathematical Moldelling of Molten Steel Flow in a Whole Degasser during RH Refining Process. *Ironmaking and Steelmaking*. 2005; 32: 427-434.
[10] L Zhang, B Rietow, K Eakin, BG Thomas. Large inclusions in plain-carbon steel ingots cast by bottom teeming. *ISIJ Inter*. 2006: 46.
[11] Y Miki, S Takeuchi. Internal Defects of Continuous Casting Slabs Caused by Asymmetric Unbalanced Steel Flow in Mold. *ISIJ Int*. 2003; 43: 1548-1555.
[12] T Lee, HJ Kim, BY Kang, SK H-wang. Effect of inclusion size on the nucleation of acicular ferrite in weld. *ISIJ Int*. 2000; 40: 1260.
[13] H Yin, H Shibata, T Emi, M Suzuki. Characteristics of agglomeration of various inclusion particles on molten steel surface. *ISIJ Int*. 1997; 37: 946–955.
[14] HJ Schulze. in Developments in Mineral Processing. 1984; 4: 65-66.
[15] L Wang, HG Lee, P Hayes. Prediction of the Optimum Bubble Size for Inclusion Removal from Molten Steel by Flotation. *ISIJ Int*. 1996; 36: 7-16.
[16] X Zheng, P Hayes, HG Lee. *ISIJ Int*. 1997; 37: 1091-1097.
[17] N Ahmed, GJ Jamson. Mineral Processing and Extractive Metallurgy Review. *Metall. Rev*. 1989; 5: 77-99.
[18] Y Sahai, T Emi. Criteria for water modeling of melt flow and inclusion removal in continuous casting tundishes. *ISIJ Int.* 1996; 36: 1166–1173.
[19] RM Wellek, AK Agrawal, AHP Skelland. Shape of liquid drops moving in liquid media'. *AIChE J*. 1966; 12: 854-862.
[20] Y Sahai, RIL Guthrie. Hydrodynamics of gas stirred melts: Part I. Gas/liquid coupling. *Metallurgical Transactions B*. 1982; 13: 193-202.
[21] H Tokunaga, M Iguchi, H Tatemichi. Turbulence structure of bottom-blowing bubbling jet in a molten Wood's metal bath. *Metallurgical and Materials Transactions B.* 1999; 30: 61-66.
[22] M Iguchi, H Tokunaga, H Tatemichi. Bubble and liquid flow characteristics in a wood's metal bath stirred by bottom helium gas injection. *Metallurgical Transactions B*. 1997; 28: 1053-1061.
[23] LF Zhang, S Taniguchi, K Matsumoto. Water model Study on Inclusion Removal from Liquid Steel by Bubble Flotation under Turbulent Conditions. *Ironmaking and Steelmaking*. 2002; 29: 326–336.
[24] LF Zhang, Jun A, Brian GT. Inclusion Removal by Bubble Flotation in a Continuous Casting Mold. *Metallurgical and Materials Transaction B*. 2006; 37B: 361–379.
[25] Indrawati I, Irmeilyana I, Fitri MP, Meiza PL. Cobb-Douglass Utility Function in Optimizing the Internet Pricing Scheme Model. *TELKOMNIKA Telecommunication Computing Electronics and Control.* 2014; 12(1): 227-240.
[26] HuiLai S, Chun J, Shuyang Z, Haiyong T. Evaluation Research of Traction Motor Performance for Mine Dump Truck Based on Rough Set Theory. *TELKOMNIKA Telecommunication Computing Electronics and Control.* 2014; 12(2): 333-342.